

# Preparation and luminescence properties of ZnO:Ga – polystyrene composite scintillator

HANA BUREŠOVÁ,<sup>1</sup> LENKA PROCHÁZKOVÁ,<sup>2</sup> ROSANA MARTINEZ TURTOS,<sup>3</sup> VÍTĚZSLAV JARÝ,<sup>4</sup> EVA MIHÓKOVÁ,<sup>4</sup> ALENA BEITLEROVÁ,<sup>4</sup> RADEK PJATKAN,<sup>1</sup> STEFAN GUNDAKER,<sup>5</sup> ETIENNETTE AUFRAY,<sup>5</sup> PAUL LECOQ,<sup>5</sup> MARTIN NIKL,<sup>4</sup> AND VÁCLAV ČUBA<sup>2,\*</sup>

<sup>1</sup>NUVIA a.s., Trojanova street 117, 278 01 Kralupy nad Vltavou, Czech Republic

<sup>2</sup>Czech Technical University in Prague, Faculty of Nuclear Sciences and Physical Engineering, Břehová street 7, 115 19 Prague, Czech Republic

<sup>3</sup>Università degli Studi di Milano Bicocca, Piazza della Scienza 3, 20126, Milano, Italy

<sup>4</sup>Institute of Physics of the AS CR, v.v.i, Cukrovarnická street 10, 162 00 Prague, Czech Republic

<sup>5</sup>CERN, 1211 Geneva 23, Switzerland

\*[vaclav.cuba@fffi.cvut.cz](mailto:vaclav.cuba@fffi.cvut.cz)

**Abstract:** Highly luminescent ZnO:Ga-polystyrene composite (ZnO:Ga-PS) with ultrafast subnanosecond decay was prepared by homogeneous embedding the ZnO:Ga scintillating powder into the scintillating organic matrix. The powder was prepared by photo-induced precipitation with subsequent calcination in air and Ar/H<sub>2</sub> atmospheres. The composite was subsequently prepared by mixing the ZnO:Ga powder into the polystyrene (10 wt% fraction of ZnO:Ga) and press compacted to the 1 mm thick pellet. Luminescent spectral and kinetic characteristics of ZnO:Ga were preserved. Radioluminescence spectra corresponded purely to the ZnO:Ga scintillating phase and emission of polystyrene at 300-350 nm was absent. These features suggest the presence of non-radiative energy transfer from polystyrene host towards the ZnO:Ga scintillating phase which is confirmed by the measurement of X-ray excited scintillation decay with picosecond time resolution. It shows an ultrafast rise time below the time resolution of the experiment (18 ps) and a single-exponential decay with the decay time around 500 ps.

©2016 Optical Society of America

**OCIS codes:** (320.0320) Ultrafast optics; (320.5390) Picosecond phenomena; (160.0160) Materials; (160.2540) Fluorescent and luminescent materials.

## References and links

1. V. A. L. Roy, A. B. Djurišić, W. K. Chan, J. Gao, H. F. Lui, and C. Surya, "Luminescent and structural properties of ZnO nanorods prepared under different conditions," *Appl. Phys. Lett.* **83**(1), 141 (2003).
2. J. Wilkinson, K. B. Ucer, and R. T. Williams, "Picosecond excitonic luminescence in ZnO and other wide-gap semiconductors," *Radiat. Meas.* **38**(4–6), 501–505 (2004).
3. V. A. Demidenko, E. I. Gorokhova, I. V. Khodyuk, O. A. Khristich, S. B. Mikhlin, and P. A. Rodnyi, "Scintillation properties of ceramics based on zinc oxide," *Radiat. Meas.* **42**(4–5), 549–552 (2007).
4. R. Li, G. R. Fern, R. Withnall, J. Silver, P. Bishop, and B. Thiebaud, "Incorporation of luminescent zinc oxide nanoparticles into polystyrene," *MRS Proc.* **1509**, 1509 (2013).
5. J. J. Huang, Y. B. Ye, Z. Q. Lei, X. J. Ye, M. Z. Rong, and M. Q. Zhang, "Highly luminescent and transparent ZnO quantum dots-epoxy composite used for white light emitting diodes," *Phys. Chem. Chem. Phys.* **16**(12), 5480–5484 (2014).
6. M. Cuba and G. Muralidharan, "Enhanced luminescence properties of hybrid Alq<sub>3</sub>/ZnO (organic/inorganic) composite films," *J. Lumin.* **156**, 1–7 (2014).
7. M. Abdullah, T. Morimoto, and K. Okuyama, "Generating blue and red luminescence from ZnO/poly(ethylene glycol) nanocomposites prepared using an in-situ method," *Adv. Funct. Mater.* **13**(10), 800–804 (2003).
8. G. Kiliani, R. Schneider, D. Litvinov, D. Gerthsen, M. Fonin, U. Rüdiger, A. Leitenstorfer, and R. Bratschitsch, "Ultraviolet photoluminescence of ZnO quantum dots sputtered at room-temperature," *Opt. Express* **19**(2), 1641–1647 (2011).
9. Y. Kumar, M. Herrera, F. Singh, S. F. Olive-Méndez, D. Kanjilal, S. Kumar, and V. Agarwal, "Cathodoluminescence and photoluminescence of swift ion irradiation modified zinc oxide-porous silicon nanocomposite," *Mater. Sci. Eng. B* **177**(16), 1476–1481 (2012).
10. V. O. Pankratov, A. L. Nylandsted, and B. N. Bech, "ZnO nanocrystals/SiO<sub>2</sub> multilayer structures fabricated by RF-magnetron sputtering," *Physica B* **404**(23–24), 4827–4830 (2009).

11. P. Thiyagarajan, M. Kottaisamy, N. Rama, and M. S. Ramachandra Rao, "White light emitting diode synthesis using near ultraviolet light excitation on Zinc oxide–Silicon dioxide nanocomposite," *Ser. Mater.* **59**(7), 722–725 (2008).
12. L. Procházková, T. Gbur, V. Čuba, V. Jarý, and M. Nikl, "Fabrication of highly efficient ZnO nanoscintillators," *Opt. Mater.* **47**, 67–71 (2015).
13. E. D. Bourret-Courchesne, S. E. Derenzo, and M. J. Weber, "Development of ZnO:Ga as an ultra-fast scintillator," *Nucl. Instrum. Meth. A* **601**(3), 358–363 (2009).
14. Calculation was performed using the data available at <http://physics.nist.gov/PhysRefData/XrayMassCoeff/>
15. K. E. Bower, Y. A. Barbanel, Y. G. Shreter, and G. W. Bohnert, *Polymers, Phosphors and Voltatics for Radioisotope Microbatteries* (CRC Press, 2002).
16. J. Q. Grim, S. Christodoulou, F. Di Stasio, R. Krahne, R. Cingolani, L. Manna, and I. Moreels, "Continuous-wave biexciton lasing at room temperature using solution-processed quantum wells," *Nat. Nanotechnol.* **9**(11), 891–895 (2014).
17. P. Lecoq, "Fast Timing with Scintillators: Towards 10 ps Time Resolution? Invited talk at SCINT2015 conference, June 8-12, 2015, Berkeley, USA
18. A.-L. Bulin, A. Vasil'ev, A. Belsky, D. Amans, G. Ledoux, and C. Dujardin, "Modelling energy deposition in nanoscintillators to predict the efficiency of the X-ray-induced photodynamic effect," *Nanoscale* **7**(13), 5744–5751 (2015).
19. A. E. Raevskaya, Ya. V. Panasiuk, O. L. Stroyuk, S. Ya. Kuchmiy, V. M. Dzhagan, A. G. Milekhin, N. A. Yeryukov, L. A. Sveshnikova, E. E. Rodyakina, V. F. Plyusnin, and D. R. T. Zahn, "Spectral and luminescent properties of ZnO–SiO<sub>2</sub> core–shell nanoparticles with size-selected ZnO cores," *RSC Advances* **4**(108), 63393–63401 (2014).
20. L.-Y. Chen, J.-Q. Xu, H. Choi, H. Konishi, S. Jin, and X.-Ch. Li, "Rapid control of phase growth by nanoparticles," *Nat. Commun.* **5**, 3879 (2014).

## 1. Introduction

ZnO is a wide direct band gap (~3.3 eV) semiconductor with high exciton binding energy (60 meV), ultrafast excitonic photoluminescence decay and strong room temperature defect related luminescence [1,2]. It typically occurs in the hexagonal (wurtzite) form. ZnO powders, thin films, quantum wells, wires or dots became intensively studied due to the number of emerging applications, namely those in optoelectronics, where it could be used. While the optically transparent scintillating ceramics has been successfully prepared from ZnO nanoparticles, the ceramization of hexagonal ZnO is not an easy task [3]. Therefore, high attention is devoted to preparation of various thin film or composite materials where scintillating (nano)particles are incorporated into the optically transparent matrix of organic or inorganic origin. Such composite materials are easier to prepare when compared to single crystals or optical ceramics. Moreover, synergies between the host matrices and the embedded powders, which can positively influence overall scintillation efficiency, are not excluded and therefore intensively searched.

Generally, the organic matrices are easy to work with and there are several papers published on the luminescent properties of ZnO embedded into the transparent organic materials. A composite sheets consisting of light emitting nano-ZnO:Zn embedded in clear polystyrene matrix prepared by a solvent casting method were reported [4] and the luminescent properties of the nanoparticles were preserved after the embedding. Similarly, highly luminescent and transparent ZnO quantum dots–epoxy composite for white light emitting diodes was prepared by a one-step precipitation using epoxy silane as a modifier and stabilizer [5]. At 8 wt %, the ZnO QDs–epoxy nanocomposite was still highly transparent and luminescent. ZnO-tris-(8-hydroxyquinoline) aluminum (Alq<sub>3</sub>) composites with varying weight fractions of ZnO in amorphous Alq<sub>3</sub> were synthesized and coated onto a glass substrate using the dip coating method. It was found that the highest intensity of greenish-blue PL emission at 485 and 514 nm was obtained at rather high ZnO content of 30 wt% [6]. Similarly, in situ growth of ZnO nanoparticles in a poly(ethylene glycol) (PEG) matrix resulted in the formation of ZnO-polymer composites with stable luminescence in blue region at 465 nm [7]. Aside from the luminescence shift, it was found out that the surplus of one of the reaction precursors – LiOH, led to more intense luminescence.

Inorganic matrices, usually amorphous or crystalline silica based materials, provide good mechanical and chemical stability and allow for various methods of ZnO incorporation, such as sputtering. Preparation of ZnO nanocrystals (quantum dots) embedded in amorphous silica was reported [8]. The composite samples were prepared without annealing in one step

sputtering process. Photoluminescence and transmittance of the composite show a shift of ultraviolet emission and absorption edge of the dots compared to bulk ZnO material. Wet electrochemical etching of porous silicon with subsequent ZnO deposition by magnetron sputtering was also used for the preparation of zinc oxide- porous silicon nanocomposites. Both white light and UV emission were observed simultaneously via photo- and cathodoluminescence spectroscopy [9]. Another method for the production of ZnO nanocrystals embedded in a SiO<sub>2</sub> matrix included radiofrequency magnetron sputtering deposition using ZnO and SiO<sub>2</sub> targets. The resulting multilayer composites consisting of ZnO/SiO<sub>2</sub> bilayers were deposited on Si substrate wafers either in vacuum or in an oxygen-rich ambience. Subsequently, the structures were heat-treated at different temperatures and in different atmospheres. PL emission in visible and UV regions were tentatively attributed to bound exciton and donor-acceptor pair recombinations, and they were similar to the corresponding lines observed in the bulk ZnO [10]. White light emitting zinc oxide-silicon dioxide nanocomposite synthesized by sol-gel combustion method showed an intense photoluminescence in near UV and visible (bluish) spectral regions with characteristics similar to those of commercial white LED diodes [11].

As summarized above, various techniques of ZnO-matrix nanocomposite preparations were developed. However beside the UV excitonic emission, obtained materials also feature intense defect related visible luminescence. Consequently, their time response includes rather slow decay components as well. This may be useful for some applications (such as white LEDs), while it prohibits the application of studied materials in fast scintillation detectors. Therefore, it is the aim of this paper to report the preparation of highly luminescent composite consisting of ultrafast ZnO:Ga scintillating powder, incorporated into the scintillating polystyrene matrix. The preparative method used allows for homogenous incorporation of ZnO:Ga nanopowder in the host matrix. Moreover, the efficient non-radiative energy transfer from the host matrix towards ZnO:Ga is evidenced.

## 2. Experimental

The highly luminescent ultrafast ZnO:Ga powder (linear crystallite size 80-100 nm, size of the particle agglomerates ~1 μm) was prepared using photochemical method described in detail elsewhere [12]. Commercially available ZnO (Aldrich, 99.999% trace metal basis) was dissolved in aqueous solution of formic acid (Penta, p.a.) with gallium (gallium nitrate, Aldrich, 99.999% trace metal basis) and hydrogen peroxide (Penta, p.a.) added. The solution was irradiated by monochromatic 254 nm UV light, until the finely dispersed nanocrystalline zinc peroxide was formed. After the thermal decomposition of ZnO<sub>2</sub> and recrystallization of ZnO:Ga at 250°C, the nanopowders were calcined at 1000°C in air and subsequently annealed at 800°C in reducing atmosphere of Ar/H<sub>2</sub> (10:1) according to [13]. Ga-doping combined with annealing in reducing atmosphere is known to enhance the fast sub-nanosecond exciton-based emission of ZnO, while slower defect-related visible emission becomes completely suppressed.

ZnO:Ga-polystyrene composite (ZnO:Ga-PS) was prepared as follows. 5 g of ZnO:Ga powder was mixed with 50 g of polystyrene (Synthos PS GP 171) in Brabender lab mixer. The mixture was then press compacted in stainless steel frame, which was placed between the pairs of glass and stainless steel slabs, into the thin 1mm thick foil. Subsequently, a pellet of 25 mm diameter was cut from the foil.

Photos of the as-prepared composite samples were taken. Scintillation properties of both free standing ZnO:Ga powder and ZnO:Ga-polystyrene composite were evaluated by measuring the radioluminescence (RL) spectra and photoluminescence (PL) decay using the custom made spectrofluorometer 5000M, Horiba Jobin Yvon, equipped with the X-ray tube (40 kV used to measure RL spectra) and nanoLED 339 nm (2 ns full-width-at-half-maximum (FWHM) pulse used to measure PL decays) excitation sources. Detection part of the set-up includes a single grating monochromator and photon counting detector TBX-04. Time-correlated single photon counting technique was utilized to measure sub-nanosecond PL decays and convolution procedure was applied (SpectraSolve software package, Ames

Photonics) to extract true decay times from exponential approximations. Measured spectra were corrected for the spectral dependence of detection sensitivity. Bismuth germanate (BGO) single crystal was used in the form of 7x7x1 mm polished plate as a reference scintillator.

Time resolved measurements under pulsed X-ray excitation up to 40 keV were performed at CERN using a Hamamatsu streak camera with the 18 ps time resolution. X-rays are triggered by a picosecond diode laser PiLAS using a repetition of 4 MHz. A delay generator provides the trigger signal for the laser and the sweeping unit in order to synchronize the light time of arrival and the ramping edge of the voltage between sweeping plates. The sample is measured in transmission geometry, building up the signal time profile in single photon counting mode. The instrumental response function (IRF) of the system has been determined measuring the laser time profile recorded by streak camera under the same measurement settings, optical path and photocathode slit aperture. The result for 100  $\mu\text{m}$  slit aperture is a Gaussian function of 127 ps FWHM which is then convoluted with the x-ray tube time profile providing FWHM of 134 ps. Measurements are corrected by 5 ns sweeping range non-linearity and background subtraction arising from the MCP noise having a signal/noise ratio around 10.

### 3. Results and discussion

The composite ZnO:Ga-PS sample appearance is shown in Fig. 1 (a). Its opaqueness is due to the thickness of the sample, high fraction of nanoparticles (10 wt% of ZnO:Ga in polymer matrix), and partial agglomeration of nanoparticles into micrometer size aggregates. Thinned sample down to 0.17 mm appears well transparent, Fig. 1 (b).

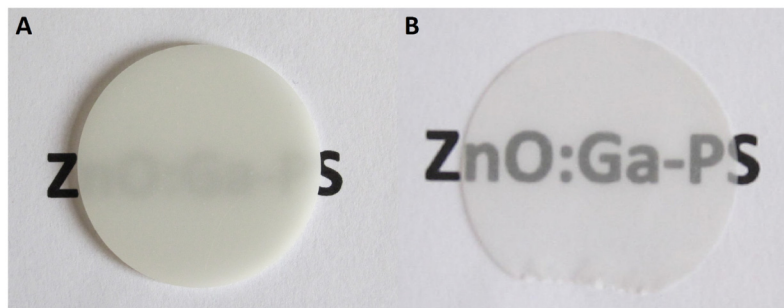


Fig. 1. Image of (a) 1 mm and (b) 0.17 mm thick ZnO:Ga-PS composite with the 10 wt% fraction of ZnO:Ga.

Luminescence properties of self-standing powder are shown in Figs. 2(a) and 2(b). The RL spectra [Fig. 2(a)] show only the narrow peak of UV excitonic luminescence, with maximum at 391 nm and the emission amplitude about three times of that of powdered BGO standard. No defect-related emission is present in the spectra. PL decay excited at 339 nm [Fig. 2(b)] exhibits the decay time about 500 ps, with no slower component present, which is demonstrated by a single exponential fit.

Absorption, photoluminescence excitation (PLE) and radioluminescence (RL) spectra of pure polystyrene scintillator used as a host matrix are displayed in Fig. 3(a). It is shown that the polystyrene scintillator itself has the absorption edge at 300 nm and narrow luminescence peak at 300-350 nm. Figure 3(a) shows that the polystyrene is suitable as the host matrix for ZnO:Ga, as it is transparent for its luminescence and ZnO:Ga intrinsic (band-to-band) absorption extending up to 370 nm, see Fig. 4(b) below, overlays most of the polystyrene emission band. The inset of Fig. 3(a) shows the absolute comparison of RL spectra of polystyrene scintillator (PS) itself and BGO single crystal plates of the same thickness. PL decay of the polystyrene scintillator is shown in Fig. 3(b). Single exponential fit provides the decay time of 11.8 ns.

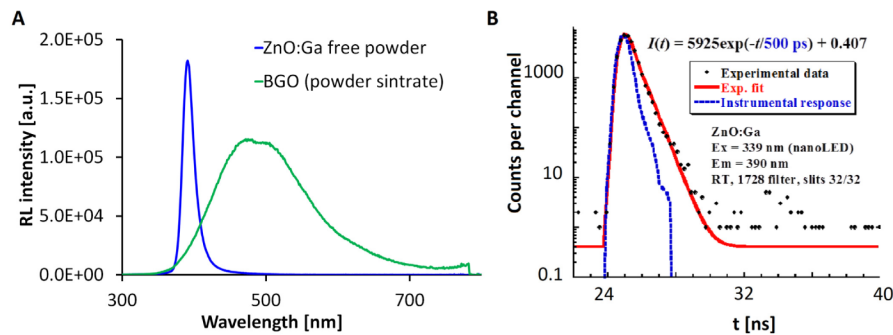


Fig. 2. A - RL spectra of ZnO:Ga free standing powder and BGO reference scintillator; B - PL decay of ZnO:Ga free standing powder. Instrumental response is also shown. Solid line is a convolution of instrumental response and the function  $I(t)$  displayed in the figure.

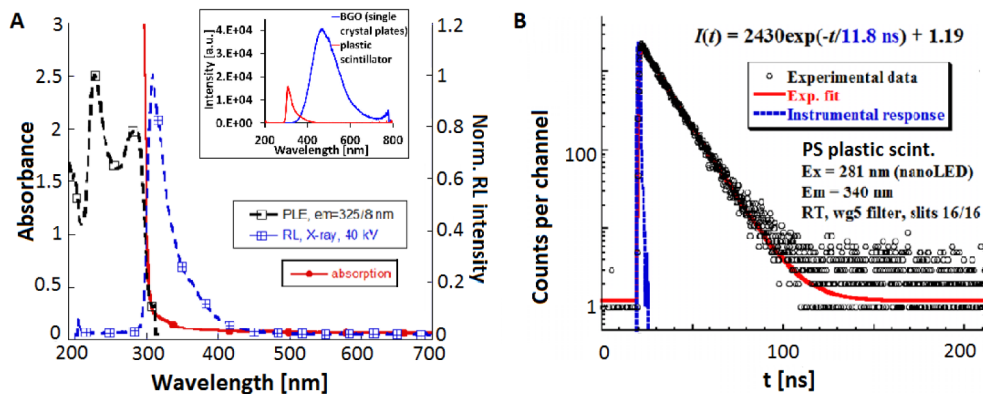


Fig. 3. A - Absorption, photoluminescence excitation (PLE) and radioluminescence (RL) spectra of polystyrene matrix (with no ZnO:Ga powder added). In the inset, absolute comparison of RL spectra of PS and BGO single crystal plates of the same thickness; B - PL decay of polystyrene matrix (with no ZnO:Ga powder added). Instrumental response is also shown. Solid line is a convolution of instrumental response and the function  $I(t)$  displayed in the figure.

Radioluminescence and absorption spectra of the ZnO:Ga-PS sample in Figs. 4(a) and 4(b) are shown in an absolute comparison with the reference powdered BGO scintillator. Absolute comparison of strongly opaque PS-ZnO:Ga composite with powdered BGO is acceptable due to similar light scattering conditions and the fact that the measurement is done in the reflection geometry. Luminescence of the composite is identical to the spectrum of ZnO:Ga in Fig. 2(a) with the maxima at 391 nm. Notably, the emission of polystyrene at 300-350 nm is absent, possibly due to the non-radiative energy transfer to ZnO:Ga or its reabsorption by the ZnO phase, as shown in Fig. 5.

It is worth comparing scintillation efficiencies of the ZnO:Ga-PS and pure PS samples in a more quantitative way. First, scintillation efficiency is proportional to the area under the RL spectra in Fig. 4(a) and the inset of Fig. 3(a). Absolute comparison of integrated RL spectra of PS and ZnO:Ga-PS with that of the standard BGO sample (also reported in respective figures) provides the scintillation efficiencies 10% of BGO and 14% of BGO, respectively.

Second, one has to take into account a possibility of incomplete absorption of X-ray excitation photons. The mean photon energy of X-ray at the 40 kV tube voltage is about 15 keV. For the 15 keV photon the attenuation coefficient of composite ZnO:Ga-PS sample (calculated density of 1.5 g/cm<sup>3</sup>) and pure PS (density 1.05 g/cm<sup>3</sup>) is 5.95 cm<sup>-1</sup> and 0.77 cm<sup>-1</sup>, respectively [14]. Thus, in 1 mm thick plates, about 45% and 7% of the 15 keV photon energy is absorbed, respectively. Therefore, about 6 times less of X-ray energy is absorbed in the PS

sample compared to the composite sample. Consequently, also the relative LY (radioluminescence intensity) of pure PS compared to composite ZnO10%:PS sample reported above is underestimated about 6 times.

When scintillation efficiencies (obtained from integrated RL spectra) reported above are corrected to an incomplete absorption one would obtain the scintillation efficiency of PS about 4 times higher than that of the ZnO:Ga-PS composite sample.

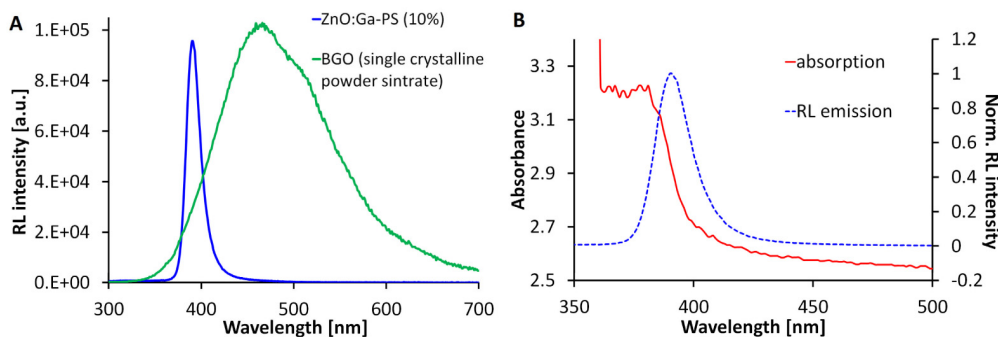


Fig. 4. A – RL spectra of ZnO:Ga-PS at room temperature, absolute comparison of the nanocomposite to the single crystalline powder BGO reference scintillator; B – absorption and normalized RL spectra of the ZnO:Ga-PS composite.

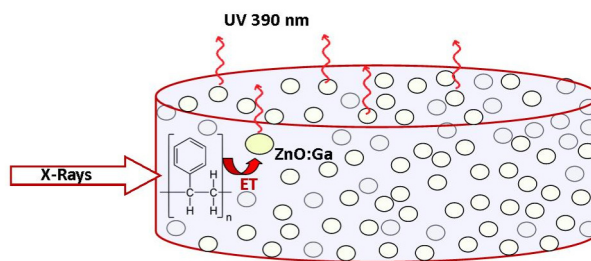


Fig. 5. Non-radiative energy transfer between polystyrene matrix and ZnO:Ga

PL decays under 339 nm excitation, which is absorbed directly in ZnO, and under 281 nm where the excitation energy is absorbed predominantly in the polystyrene matrix, are shown in Figs. 6(a) and 6(b). In the case of 339 nm excitation, the decay is virtually sub-nanosecond, slight non-exponentiality might be caused by the energy loss during the transfer from ZnO structure to the defects at the interface with the polystyrene matrix. In the case of 281 nm excitation, the sub-nanosecond component is again predominant (cca 92%). Based on comparison with Fig. 2(d), the minor slower component with  $\sim 10$  ns decay can probably be attributed to the decay of polystyrene matrix. In both Figs. 6(a) and 6(b), the kinetics of PL decay is sub-nanosecond and corresponds to the decay of ZnO:Ga, shown in the Fig. 2(b). Such decay characteristics strongly suggest the effective non-radiative energy transfer from polystyrene to ZnO:Ga. The resulting nanocomposite is therefore faster than the original plastic scintillator; ZnO:Ga embedding also somewhat increases the density and the effective atomic number of the composite.

It is worth noting the quantum yield of photoluminescence centers in PS and ZnO:Ga at room temperature. In case of PS it is close to one (for plastic scintillators scintillation efficiency decreases typically only by  $-0,1$  up to  $-0,3\%/^{\circ}\text{C}$  within an interval from  $-33$  to  $+67^{\circ}\text{C}$  [15]) and the photoluminescence decay time of PS in Fig. 3(b) is nearly constant within this temperature range (data not shown) as well. Quantum yield of ZnO:Ga luminescence, however, is certainly much less than 1 at room temperature. It follows from its temperature dependence [12]. The amplitude of fast near UV emission band at room temperature with respect to that at 8K decreases by about one and half order of magnitude. The difference of

scintillation efficiencies between the composite and PS sample is, however, not that high. The point is that scintillation efficiency of nano or microcrystals of direct gap semiconductors as ZnO is severely affected by the surface conditions, perfection and nonradiative traps present. At this point, it is difficult to quantitatively compare literature data for free standing ZnO:Ga powder and the present composite sample in which the ZnO:Ga nanophase is surrounded by or even embedded into polystyrene host.

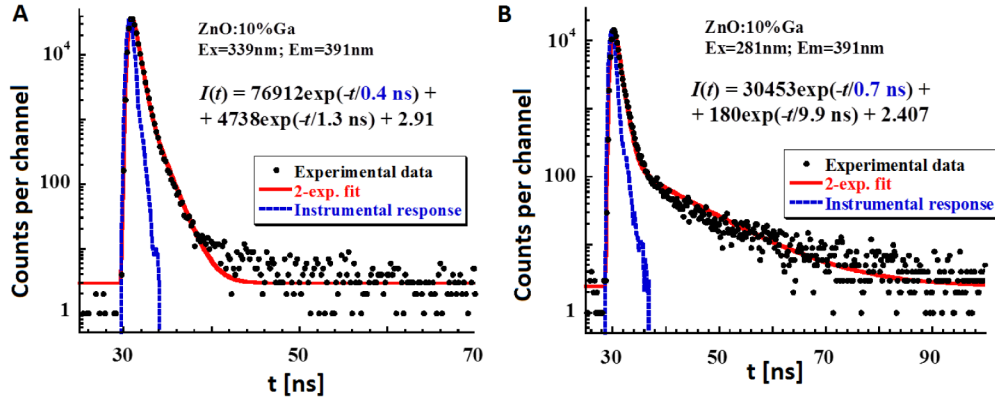


Fig. 6. A – PL decay at the excitation by the nanoLED source, ex = 339 nm. B – PL decay at the excitation by the nanoLED source, ex = 281 nm. Instrumental response is also shown. Solid line is a convolution of instrumental response and the function  $I(t)$  in the figure.

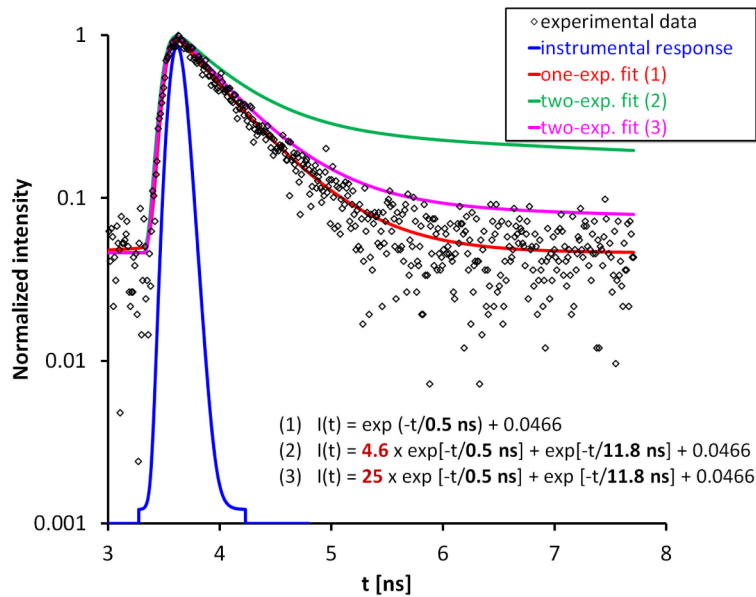


Fig. 7. Spectrally unresolved scintillation decay of PS-ZnO:Ga composite under the picosecond X-ray pulse excitation,  $U = 40 \text{ kV}$ . Instrumental response (IRF) is also shown in the figure. Lines (1), (2) and (3) are convolutions of IRF and functions  $I(t)$  displayed in the figure, for details, see the text.

In Fig. 7 the scintillation decay of ZnO:Ga-PS composite sample under picosecond X-ray pulse excitation is shown. Within the achieved signal-to-background ratio which is about 25, there is no slow component resolvable in the decay. The decay time of 0.5 ns calculated from a single exponential approximation (curve (1)) is identical to the values reported above for the PL decay of the ZnO:Ga nanopowder. No distinguishable rising time in the decay

approximation (inclusion of a rising component into  $I(t)$  does not improve the quality of the fit) means that it is below the time resolution limit of the set-up (18 ps). Such observation confirms negligible delay in the transport stage of scintillation mechanism in the composite sample and suggests such a material as being suitable in sandwich (phoswich) scintillators in time-of-flight measurements to maximize timing coincidence resolution similarly to other quantum dot materials which are under development for this purpose [16,17].

Figure 7 together with Fig. 6(b) provides firm support for the claim that an efficient and fast non-radiative energy transfer takes place from PS host towards ZnO:Ga nanocrystals. We note that modelling the energy deposition in qualitatively similar composite system [18] shows that overall energy deposition in homogeneously dispersed scintillator nanophase in water is close to its volume fraction under the excitation by X-ray from a few keV up to hundreds of keV. Thus, in our case we expect that under X-ray excitation used in Fig. 7 only 10-20% of the absorbed X-ray energy is deposited in ZnO:Ga scintillating nanophase, while its major part, 80-90%, is absorbed in PS host. As the scintillation efficiencies of PS and ZnO:Ga appear comparable from their radioluminescence spectra shown in Figs. 2(a) and 3(a), the purely radiative energy transfer from PS to ZnO:Ga would fingerprint the photoluminescence decay component (10-12 ns) of PS into that of ZnO:Ga with the expected overall weight in the scintillation decay in Fig. 7 of about 80-90%.

Let us express these considerations quantitatively. The kinetic equations describing the time evolution of excited state populations  $N_1$ ,  $N_2$  of ZnO:Ga phase (state 1) and PS host (state 2), respectively, with no energy transfer between them are:

$$\begin{aligned} dN_1 / dt &= -k_1 N_1 \\ dN_2 / dt &= -k_2 N_2 \end{aligned} \quad (1)$$

where  $k_1$ ,  $k_2$  denote the radiative decay rates (inverse decay times) from excited states 1 and 2 to the ground state, respectively.

Radiative transfer from PS to ZnO:Ga can be introduced using a factor  $f$  from the interval  $\langle 0,1 \rangle$  where  $f = 0$  represents no reabsorption of PS luminescence by ZnO:Ga, while  $f = 1$  indicates total reabsorption. The kinetic equations now read:

$$\begin{aligned} dN_1 / dt &= -k_1 N_1 + k_2 N_2 f \\ dN_2 / dt &= -k_2 N_2 (1 - f) - k_2 N_2 f = -k_2 N_2 \end{aligned} \quad (2)$$

The solution of the system (2) provides populations  $N_1(t)$  and  $N_2(t)$  and consequently the total decay intensity  $I(t) = k_1 N_1(t) + k_2 (1-f) N_2(t)$ . For the total reabsorption  $f = 1$  and initial 20% energy deposition in the ZnO:Ga phase under X-ray excitation the function  $I(t)$  becomes

$$I(t) = 4.6 \times \exp(-t/0.5 \text{ ns}) + \exp(-t/11.8 \text{ ns}) \quad (3)$$

Equation (3) is convoluted with the instrumental response and displayed as the curve no. (2) in Fig. 7. The curve no. (3) in Fig. 7 is calculated for the case of  $f = 1$  when the amplitude ratio of the fast-to-slow components is 25, i.e. comparable with the signal-to-background ratio. Such ratio can only be reached at the situation when electrons and holes generated in PS are partially transferred to ZnO:Ga before they reach a relaxed excited state (and radiation would take place) in PS, i.e. the initial energy deposition is different from 20% in ZnO:Ga. In particular, it has to be 54% in ZnO:Ga. In both cases (curves no. (2) and (3)) the slow component is clearly resolved from the background. The slow component becomes truly indistinguishable from the background for initial deposition of about 92% in ZnO:Ga (the fast-to-slow ratio about 260).

The same exercise can be done for PL decay in Fig. 6b, considering that under the 281 nm excitation both PS and ZnO:Ga are excited band-to-band. Provided an oscillator strength of these intrinsic band-to-band transitions is comparable in both materials and given the volume fraction, about 10% of excitation energy should be deposited in ZnO:Ga. However, considering the decay function  $I(t)$  in Fig. 6b (the amplitude ratio of the fast and slow



component is about 170), the initial energy deposition would need to be about 88% in ZnO:Ga. Here, we note that the radiative energy transfer might predominantly arise in local regions where ZnO:Ga nanophase occurs at lower volume fractions due to local inhomogeneities.

Taking into account the values reported above, it is obvious that the radiative energy transfer (if any) represents very minor contribution to energy transfer from PS host towards ZnO:Ga phase and the existence of fast nonradiative energy transfer from PS to ZnO:Ga is the only viable explanation. In fact, most probably, such energy transfer is realized by migration of free electrons and holes from PS into ZnO:Ga, even before they form a relaxed excited state in PS. It follows from the evaluation of the decays in Fig. 6b and 7 that about 90% of energy initially deposited in PS is nonradiatively transferred into ZnO:Ga phase. This would be an ideal situation in a composite scintillator where in picosecond time scale the energy absorbed in the host is transferred into the scintillating nanophase.

The application of such an ultrafast composite scintillator based on PS-ZnO:Ga can be envisaged e.g. in the field of alpha particle detection (the penetration depth of which is about 10-20 micrometers) or low energy electron or photon (EUV, VUV) beams monitoring where such a scintillator can provide precious information for timing, e.g. in the above mentioned time-of-flight type measurements using a sandwich scintillator arrangement [17]. Even for visually discouraging opacity seen in Fig. 1 we note that a reduction of sample thickness down to 0.1 mm, will result in the measured "absorbance" in transparency region of about 0.26 - as derived from Fig. 4(b) - which means approx. 55% transparency of such a thin foil, perfectly usable in practical applications. Furthermore, the practical experience shows that a slight scattering in the volume of thin optical element actually helps guiding the light out of the element. Such a thin plastic foil can easily be handled and optically coupled with other bulk scintillator elements or photodetectors. We have also prepared a thin pellet about 0.1 mm thick by cold-pressing the ZnO:Ga powder. However, it appeared so brittle, that even under a gentle manipulation in transmission measurement it broke into pieces which disabled any other luminescence characterization. Thus, thin optical element prepared from ZnO:Ga powder in this way cannot be used in practical applications. We are working on better suppression of agglomeration of ZnO:Ga nanoparticles in PS host using a core-shell strategy [19] or even a self-organized nanoparticle layer around ZnO:Ga nanocrystals [20]. The latter could provide even more effective chemical bonding with the host. These studies are, however, outside of the scope of the present paper and will be reported in our future work.

#### 4. Conclusions

Highly luminescent nanocomposite of ZnO:Ga powder embedded in polystyrene scintillating matrix was successfully prepared, with the 10 wt% fraction of ZnO:Ga. Separately, each of the ZnO:Ga and polymer matrix shows its characteristic luminescence properties. However, the composite retains the desirable properties of ZnO:Ga, i.e. its intense excitonic luminescence in the near UV spectral range and ultrafast sub-nanosecond PL decay. The interaction between the matrix and ZnO:Ga seems to positively influence the scintillating properties. RL emission spectra correspond to the pure ZnO:Ga scintillating phase, emission of polystyrene at 300-350 nm is absent. The dominance of ultrafast subnanosecond decay component even under the band-to-band excitation into the polystyrene host or picosecond X-ray pulse excitation shows that the fast and effective non-radiative transfer from polystyrene host towards ZnO:Ga scintillating nanophase occurs. In picosecond time scale this energy transfer pathway brings at least 90% of energy, initially deposited in PS, into ZnO:Ga. Moreover, such a flexible and easy-to-use plastic foil can be exploited in practical applications and coupled with another fast and high-light-yield inorganic scintillator to further enhance its capabilities for fast timing.

#### Acknowledgments

This article is based upon work from COST Action (TD1401, FAST), supported by COST (European Cooperation in Science and Technology) and EC H2020-TWINN-2015 no. 690599

(ASCIMAT) and the ERC Advanced Grant no. 338953 (TICAL) and was performed in the frame of Crystal Clear Collaboration. The authors also gratefully acknowledge the support by the Grant Agency of the Czech Republic, grant no. GA13-09876S and by the Grant Agency of the Czech Technical University in Prague, grant No. SGS14/207/OHK4/3T/14.